ELSEVIER

Bis-silyl substituted ferrocenylenes, including dicyanovinyl electron-withdrawing groups, as potential non-linear optical materials

Xiaoming Zhao [a], Hemant K. Sharma [a], Francisco Cervantes-Lee [a], Keith H. Pannell [a],*, Gary J. Long [b], Ahmed M. Shahin [b]

[a] *Department of Chemistry, University of Texas at El Paso, 500 W. University Avenue, El Paso, TX 79968-0513, USA*
[b] *Department of Chemistry, University of Missouri- Rolla, Rolla, MO 65409-0010, USA*

Abstract

1,1′-Bis-silylferrocenylenes (p-$XC_6H_4SiMe_2$-$C_5H_4)_2Fe$, X = Br (**1**), CHO (**2**), CH=C(CN)$_2$ (**3**) have been synthesized and characterized by NMR and Mössbauer spectroscopy, single crystal X-ray diffraction and electrochemistry. Complex **1** crystallizes in the centrosymmetric space group $P2_1/n$ whereas **3** forms in the non-centrosymmetric group Cc. The latter complex exhibits a chain-like structure in the solid state via C−H···N intermolecular hydrogen bonding. The hyperpolarizability of **3** is significantly greater than the related mono-silylferrocene complex $(C_5H_5)Fe(C_5H_4SiMe_2C_6H_4CH=C(CN)_2)$ while Mössbauer spectroscopy exhibits negligible charge transfer between the cyano groups and the ferrocenylene iron center.
© 2003 Published by Elsevier B.V.

Keywords: Ferrocenylenesilyl; NLO; Mössbauer

1. Introduction

Organometallic compounds consisting of conjugated donor–acceptor systems have been shown to possess large second order non-linearities [1]. There has been considerable interest in the use of ferrocene as a donor group [2] in the synthesis of potentially non-linear optical materials since Green in 1987 demonstrated that ferrocene connected via an ethylene linkage to an acceptor moiety had an excellent second harmonic generation (SHG) efficiency [3]. Zyss et al. reported the second-order optical non-linear properties with a wide range of transparency of the donor–acceptor compounds linked via oligosilanes [4]. Previous studies from our laboratories on mono-substituted ferrocenyloligosilanes show weak ferrocene–aryl interactions through the silicon chain [5], and this observation has been verified by other groups [6]. Despite these rather unimpressive results we continue our quest for new

materials with better non-linear optical properties and now report the synthesis, characterization, electrochemistry, Mössbauer spectra and non-linear optical properties of new 1,1′-bis(silyl)ferrocenylenes.

2. Results and discussion

Treatment of 1,1′-dilithioferrocene with (p-bromophenyl)chlorodimethylsilane at −25 °C in THF resulted in the formation of bis-bromoferrocenylene derivative **1** in 17% yield. The subsequent reaction of **1** with t-BuLi at −78 °C followed by the addition of DMF provided orange crystals of **2** in 45% yield. Knoevenagel condensation of **2** with malanonitrile resulted in the formation of **3** in 60% yield an air-stable red crystalline solid. The synthetic sequence is shown in Scheme 1 [5,6].

An important feature of the ^{1}H-NMR spectra of the bis-substituted ferrocenylenes, **1**–**3**, is the small systematic low field chemical shifts of the Cp resonances in the ^{1}H-NMR spectra which is indicative of the inductive effects of the Br, −CHO and −CH=C(CN)$_2$ substituents. For example, the ^{1}H-NMR spectra of **1** and **2** show a pair of triplets (δ 3.84 and 4.06 for **1** and at δ 3.95 and

* Corresponding author. Tel.: +1-915-747-5796; fax: +1-915-747-5748.

*E-mail address:* kpannell@utep.edu (K.H. Pannell).
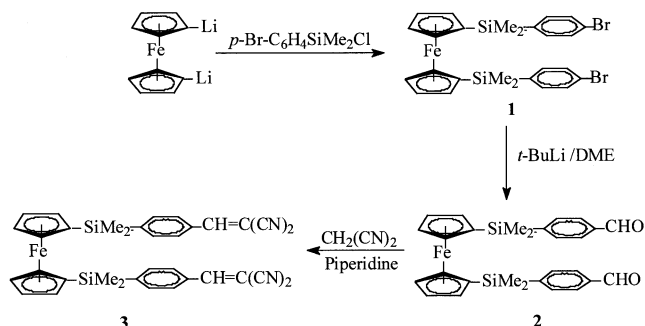
Scheme 1.

4.15 for **2**) assigned to Cp protons. Thus, the difference in chemical shifts between the C_5H_4 protons for (**1** and **2**), and (**2** and **3**), $\Delta\delta$, is 0.1 ppm clearly demonstrating the deshielding effects of the substituents on the cyclopentadienyl ring. The ^{29}Si-NMR chemical shifts for **1–3** (-6.8, -6.6 and -6.0 ppm respectively) also indicate the weak electronic effects of the substituents.

The UV–vis absorption maximum in **3** is present at 436 nm, a substantial blue shift from λ_{max} observed in **1** (453 nm in CH_2Cl_2) indicating a charge communication between ferrocene and dicyanovinyl groups.

2.1. Crystal structures for **1** and **3**

The molecular structures of **1** and **3** are shown in Figs. 1 and 2. A summary of cell constants and data collection parameters is included in Table 1. Selected bond lengths and bond angles are given in Table 2.

The most interesting and, in view of the NLO properties, the most important feature is that whereas **1** crystallized in the centrosymmetric space group $P2_1/n$, **3** is in the non-centrosymmetric space group *Cc*. As expected in both compounds the two silyl substituents on the two cyclopentadienyl rings are oriented *trans* to each other presumably minimizing the steric strain. Interestingly, **3** is an example of a molecule exhibiting the recently discussed self-assembly [7] of organometallics. In this example, two types of hydrogen bonds are
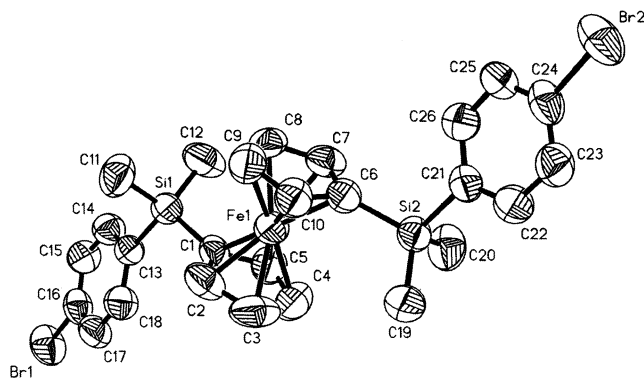
observed (Fig. 3): (a) The methyl H of the silyl group and the N_4 of the cyano group of the adjacent molecules are involved in intermolecular hydrogen bonding with interatomic distance of 2.57 Å for $C_{11}-H_{11h}\cdots N_4$. (b) The other type of C–H···N hydrogen bond involves one of the hydrogen of aromatic ring carbon C_{18} and N_1 of the cyano group with a slightly longer interatomic distance of 2.68 Å for $C_{18}-H_{18c}\cdots N_1$ bond. These two types of unconventional C–H···N hydrogen bonds give rise to a chain structure, a relatively rare type of H-bonding. The C–H...N interatomic distances are shorter than that observed in C–H···N hydrogen-bonded pyridine derivatives (3.37–3.44 Å) [8,9] and longer than that in 3-methyl-4-propargylthioquinoline (2.28 Å) [10]. We retrieved the atomic coordinates from the Cambridge Crystallographic Data Base [11] for 3-methyl-4-propargylthioquinoline and reviewed the hydrogen bonding distance and found the value of 2.406 Å for C–H···N bonds probably due to hydrogen normalization in the deposited data. The hydrogen bonds are not linear and the $C_{18}-H_{18c}\cdots N_1$ and $C_{11}-H_{11h}\cdots N_4$ angles of 157° and 164° respectively are wider than those observed in the tetrakis(2-vinylpyridyl)benzene–dichloromethane [9] but the value of 157° is the same as that observed in 3-methyl-4-propargylthioquinoline [10].

2.2. Electrochemistry

Compounds **1–3** were studied by cyclic voltammetry which was performed on samples containing 10^{-3} M of the compound in 0.1 M solution of $[Bu_4N][BF_4]$ in CH_2Cl_2 at room temperature. Each compound undergoes a reversible one-electron oxidation (Table 3). Compounds **1** and **2** are oxidized at higher potential (0.1 V) in comparison with ferrocene due to the inductive effects of the $-Br$ and $-CHO$ groups. However, **3** is oxidized at a potential close to that of ferrocene and small uncharacterized species also appear at a higher oxidation potential (1.05 V). The irreversible wave in **3** at higher reduction potential (-0.6 V) is attributed to the dicyanovinyl groups and appears at a lower reduction potential than in a similar complex **4** [6b].
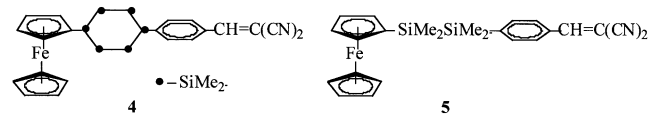
2.3. NLO properties

The preliminary results on the hyperpolarizability of **3** with a β_0 value of 57.0×10^{-30} esu indicates moderate interactions between ferrocene and dicyanovinyl portion

Fig. 1. Thermal ellipsoid (50%) drawing of **1**.
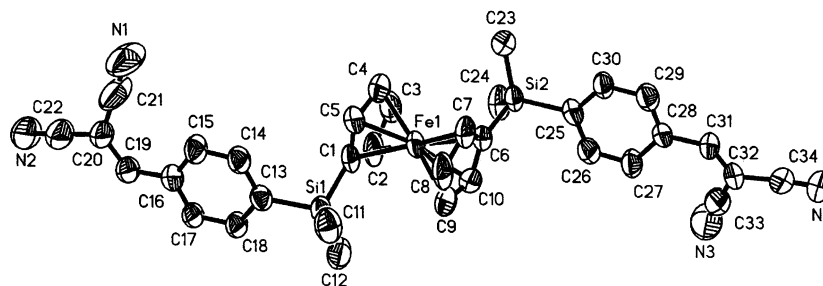
Fig. 2. Thermal ellipsoid (50%) drawing of **3**.

Table 1
Crystal data for **1** and **3**

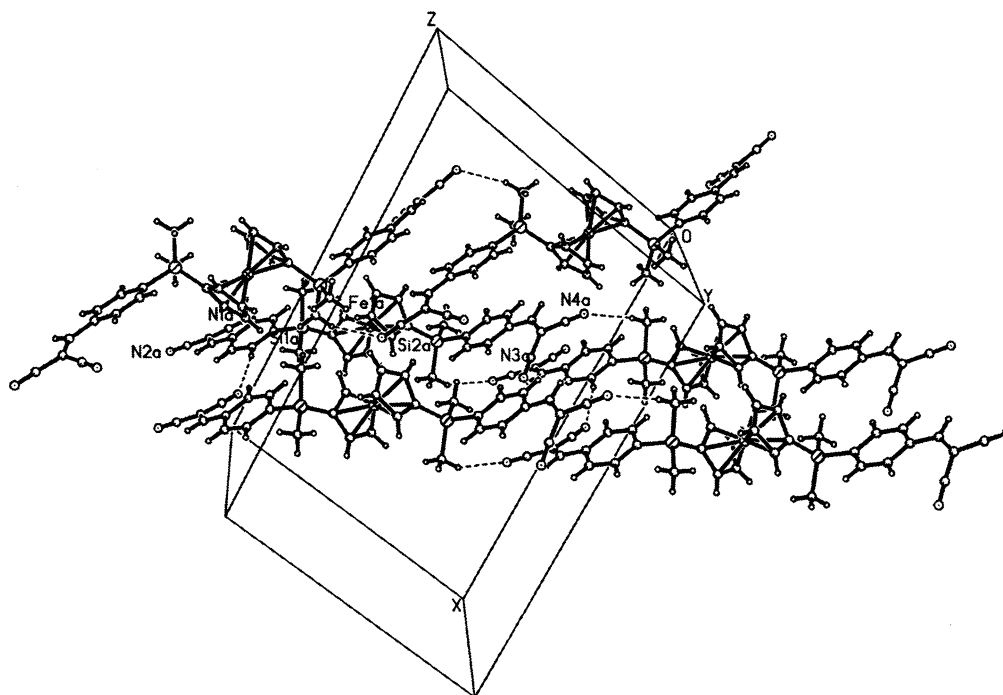| Compound	**1**	**3**
Empirical formula	$C_{26}H_{28}Br_2Si_2Fe$	$C_{34}H_{30}N_4Si_2Fe$
Color; habit	Orange fragment	Orange fragment
Crystal size (mm)	$0.80 \times 0.48 \times 0.28$	$0.60 \times 0.32 \times 0.28$
Crystal system	Monoclinic	Monoclinic
Space group	$P2_1/n$	Cc
Unit cell dimensions		
a (Å)	9.0166(2)	28.10(9)
b (Å)	16.601(3)	9.190(5)
c (Å)	17.894(4)	15.527(6)
α (°)	90	90
β (°)	98.17(2)	103.31(3)
γ (°)	90	90
V (Å³)	2651.1(10)	3167(2)
Density (g ml^{-1})	1.53	1.27
Absorption coefficient (mm^{-1})	3.69	0.58
Z	4	4
2θ Range (°)	3.5–50	3.5–50
Scan type	ω	ω
Scan speed (° min^{-1})	4–20	4–20
Scan range (ω) (°)	1.20	1.40
Standard reflections	3 measured every 197 reflections	3 measured every 197 reflections
Index ranges	$-10 \leq h \leq 0$, $0 \leq k \leq 19$, $-21 \leq l \leq 21$	$-27 \leq h \leq 27$, $-10 \leq k \leq 10$, $-18 \leq l \leq 18$
Reflection collected	4923	6488
Independent reflections	4614	4116
Observed reflections	$2580(F > 2.0\sigma(F))$	$4717 (F > 2.0\sigma(F))$
Refined parameters	280	373
Absorption correction	Semi-empirical	Semi-empirical
Min./max. transmission	0.009/0.027	0.100/0.113
Flack's parameter	–	0.085 (0.0261)
Final R indices (obs. data)	$R = 5.80\%$, $wR = 15.45\%$	$R = 5.75\%$, $wR = 16.48\%$

Table 2
Selected bond lengths (Å) and angles (°) for **1** and **3**

1

Bond lengths

Fe(1)–C(3)	2.027(9)	Si(1)–C(12)	1.853(9)
Fe(1)–C(1)	2.060(6)	Si(1)–C(11)	1.850(8)
Fe(1)–C(6)	2.064(6)	Si(1)–C(13)	1.884(7)
Fe(1)–C(9)	2.058(8)	Si(2)–C(19)	1.833(8)
Br(1)–C(16)	1.910(7)	Si(2)–C(6)	1.850(7)
Br(2)–C(24)	1.909(7)	Si(2)–C(21)	1.879(7)
Si(1)–C(1)	1.840(7)	Si(2)–C(20)	1.859(8)

Bond angles

C(1)–Si(1)–C(12)	110.3(4)	C(19)–Si(2)–C(6)	110.9(4)
C(1)–Si(1)–C(11)	109.7(4)	C(19)–Si(2)–C(21)	108.8(3)
C(12)–Si(1)–C(11)	111.5(5)	C(6)–Si(2)–C(21)	106.6(3)
C(1)–Si(1)–C(13)	108.1(3)	C(19)–Si(2)–C(20)	111.2(4)
C(12)–Si(1)–C(13)	108.5(4)	C(6)–Si(2)–C(20)	111.2(4)
C(11)–Si(1)–C(13)	108.9(4)	C(21)–Si(2)–C(20)	108.0(4)

3

Bond lengths

Fe(1)–C(8)	2.033(7)	Si(2)–C(6)	1.862(7)
Fe(1)–C(7)	2.040(7)	Si(2)–C(25)	1.879(6)
Fe(1)–C(9)	2.049(7)	Si(2)–C(23)	1.844(7)
Fe(1)–C(5)	2.042(6)	Si(2)–C(24)	1.860(9)
Fe(1)–C(10)	2.051(7)	N(1)–C(21)	1.120(13)
Si(1)–C(1)	1.856(7)	N(2)–C(22)	1.117(10)
Si(1)–C(13)	1.887(6)	N(3)–C(33)	1.138(12)
Si(1)–C(12)	1.855(7)	N(4)–C(34)	1.136(10)
Si(1)–C(11)	1.868(8)		

Bond angles

C(1)–Si(1)–C(13)	106.4(3)	C(25)–Si(2)–C(24)	108.0(3)
C(1)–Si(1)–C(12)	109.5(3)	C(23)–Si(2)–C(24)	111.1(5)
C(13)–Si(1)–C(12)	108.9(3)	N(1)–C(21)–C(20)	178.5(14)
C(1)–Si(1)–C(11)	111.0(4)	N(2)–C(22)–C(20)	178.2(10)
C(13)–Si(1)–C(11)	107.8(3)	C(32)–C(31)–C(28)	131.0(7)
C(12)–Si(1)–C(11)	113.0(4)	C(31)–C(32)–C(34)	121.0(8)
C(6)–Si(2)–C(25)	107.6(3)	C(31)–C(32)–C(33)	124.4(7)
C(6)–Si(2)–C(23)	109.9(3)	C(34)–C(32)–C(33)	114.0(7)
C(25)–Si(2)–C(23)	109.5(3)	N(3)–C(33)–C(32)	177.3(9)
C(6)–Si(2)–C(24)	110.6(4)	N(4)–C(34)–C(32)	176.7(8)

2.4. Mössbauer spectra

The use of Mössbauer spectroscopy to aid in the analysis of organoiron complexes is well established. Indeed, there have been several such studies [6] of silylferrocenes with potentially useful NLO properties. In general the observed room temperature Mössbauer

of the molecule. The hyperpolarizability of **3** is eight times greater than that of **5** ($\beta_0 = 7.0 \times 10^{-30}$ esu) [5].

Fig. 3. H-bonding scheme for self-assembly of **3**.

Table 3
Cyclic voltammetry data (V) at scan rate 50 mV s^{-1}

Compound	E_{pa}	E_{pc}	ΔE [a]
Ferrocene	0.59	0.38	0.21
1	0.69	0.55	0.14
2	0.70	0.56	0.14
3	0.60	0.50	0.10

[a] Anodic–cathodic peak separation.

spectra are in accord with the expected low-spin iron (II) character of the ferrocenyl groups as is the case at 296 K for complex **3**. However, there are some reports that such compounds exhibit Mössbauer spectra which indicate the presence of iron(III) at lower temperatures and, as a consequence, some authors have indicated that some degree of charge transfer has been observed.[6]

The Mössbauer spectra of **3** have been measured at 296 and 78 K (Fig. 4), and the resulting hyperfine parameters, based on symmetric Lorentzian quadrupole doublet fits, are given in Table 4. Although the 296 K spectrum shows the presence of an iron(III) component, this component is not apparent at 78 K. As a consequence of this absence, we attribute the weak doublet observed at 296 K to a trace of an iron(III) impurity. Although this impurity component must be present in both spectra, it is only apparent at 296 K, a temperature at which the recoil-free fraction of the iron(II) in **3** is, as expected, very small relative to that of the iron(III) trace impurity. It is well known that the recoil-free fraction of ferrocene-like iron(II) increases dramatically upon cool-
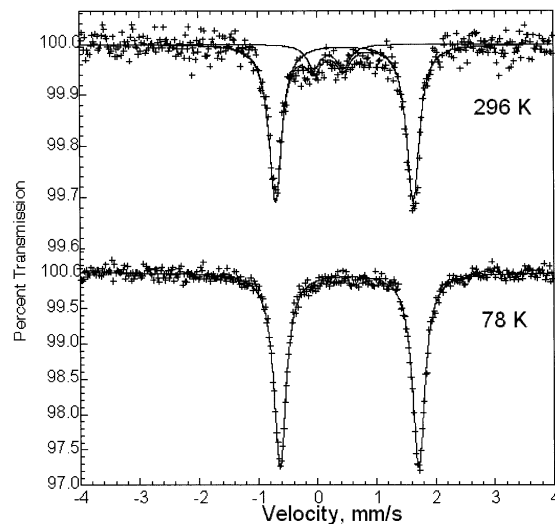
Fig. 4. Mössbauer spectra of **3**.

ing from 296 to 78 K. This is apparent in Fig. 4 as the large increase in the percent absorption between 296 and 78 K; the corresponding increase in the iron(II) spectral absorption area from 0.25 to 2.15 (%ε)/(mm s^{-1}) is indeed large. If one makes the reasonable assumption that the iron recoil-free fractions of the iron(II) in **3** and the iron(III) impurity are similar at 78 K, a fit of the spectrum indicates that the sample contains at most 0.3 weight percent of the iron as an iron(III) impurity.

Further it should be noted that the hyperfine parameters of **3** are typical of ferrocene-like complexes. Specifically, **3** exhibits a 78 K isomer shift of 0.537 mm

Table 4
Mössbauer spectral hyperfine parameters

Compound	T (K)	δ (mm s^{-1}) [a]	ΔE_Q (mm s^{-1})	Γ (mm s^{-1})	Area (%)	Area (%ε) (mm s^{-1})	Assignment
3	296	0.458	2.33	0.26	86	0.25	Iron(II)
		0.199	0.50	0.29	14	0.04	Iron(III) trace impurity
	78	0.537	2.34	0.25	100	2.15	Iron(II)
Cp$_2$Fe	295	0.447	2.40	0.23	100	–	Iron(II)
	85	0.533	2.40	0.26	100	–	Iron(II)

[a] The isomer shifts are given relative to room temperature α-iron foil.

s^{-1} and a quadrupole splitting of 2.34 mm s^{-1}. The comparable values for ferrocene [12] are 0.533 mm s^{-1} and 2.40 mm s^{-1} (see Table 4). We conclude that there is no evidence for any charge transfer which would lead to a ferrocenium-like species in **3**. The EPR spectra of **3** recorded at room temperature 300 K and at 77 K exhibit no signal due to Fe(III) component in the compound. The origin of the iron(III) trace impurity in **3** is unknown at this time and two independently synthesized samples of **3** provided exactly identical results.

3. Experimental

All syntheses were performed under a dry nitrogen atmosphere using standard Schlenk techniques. Tetrahydrofuran and hexanes were distilled over sodium and benzophenone ketal. N,N'-Tetramethylethylenediamine (TMEDA) was distilled over calcium oxide. Me$_2$SiCl$_2$ was distilled before use and stored over 4 Å molecular sieves. Dilithioferrocene was synthesized according to a literature procedure [13]. NMR spectra were recorded on Bruker 300 MHz spectrometer.

3.1. Synthesis of 1

To a stirred slurry of 1,1′-dilithioferrocene (3.76 g, 19.0 mmol) in 40 ml of THF at −25 °C was added slowly via a dropping funnel, a solution of (4-bromophenyl)chlorodimethylsilane (9.47 g, 37.94 mmol) in 40 ml of THF. The mixture was stirred at low temperature for 30 min and then warmed to room temperature (r.t.) and further stirred for 14 h. The solvent was removed under vacuum, and the orange residue was extracted into 60 ml of hexanes and filtered on Celite. The filtrate was concentrated to 10 ml and chromatographed on silica gel (80–200 mesh) column (2 × 15 cm). Elution with hexane produced an orange band that eluted to yield 2.0 g (3.26 mmol, 17%) of **1** as an orange powder, m.p. 122–124 °C. Anal. Calc. for C$_{26}$H$_{28}$Br$_2$FeSi$_2$: C, 51.00; H, 4.61. Found: C, 50.52; H, 4.66%. ^{1}H-NMR (C$_6$D$_6$): 0.29 (s, 6H, SiMe$_2$); 3.84 (t, J = 1.5 Hz, 2H, Cp), 4.06 (t, J = 1.5 Hz, 2H, Cp); 7.08–7.11 (dd, 2H, Ph), 7.25–7.28 (dd, 2H, Ph); ^{13}C-NMR (C$_6$D$_6$): −1.65 (SiMe$_2$); 69.6 (ipso), 71.9, 73.6 (Cp); 124.1, 131.2,

135.6, 138.5 (Ph); ^{29}Si-NMR (C$_6$D$_6$): −6.8; UV–vis (CH$_2$Cl$_2$): λ_{max} 453 nm.

3.2. Synthesis of 2

A 100 ml Schlenk flask was charged with 1.10 g (1.8 mmol) of **1** in 20 ml THF. To this solution, maintained at −78 °C, was added slowly via a syringe 4.72 ml t-butyl lithium (1.7 M in hexanes). The orange reaction mixture was stirred for 5 min at low temperature and then 4 ml of DMF was added. The temperature of the reaction was allowed to rise to r.t. and the reaction mixture was stirred at r.t. for 16 h. The reaction was quenched with 30 ml of satd aq NH$_4$Cl solution, the resulting mixture was extracted with 100 ml benzene. The organic layer was dried over MgSO$_4$, and the solvent was removed. Column chromatography on silica gel (hexane–benzene 50/50 v/v) yielded **2** as an orange powder, recrystallized from hexane–benzene (0.41g, 0.8 mmol, 45% yield). m.p. 96–97 °C. Anal. Calc. for C$_{28}$H$_{30}$FeO$_2$Si$_2$: C, 65.87; H, 5.92. Found: C, 65.84; H, 5.92%. ^{1}H-NMR (C$_6$D$_6$): 0.40 (s, 6H, SiMe$_2$); 3.95 (t, J = 1.5 Hz, 2H, Cp), 4.15 (t, J = 1.5 Hz, 2H, Cp); 7.46–7.48 (dd, 2H, Ph), 7.59–7.61 (dd, 2H, Ph), 9.70 (s, 1H, –CHO); ^{13}C-NMR (C$_6$D$_6$): −1.84 (SiMe$_2$); 69.2 (ipso), 72.1, 73.7 (Cp); 128.7, 134.4, 137.1, 147.7 (Ph), 191.8 (CHO); ^{29}Si-NMR (C$_6$D$_6$): −6.6; UV–vis (CH$_2$Cl$_2$): λ_{max} 434 nm.

3.3. Synthesis of 3

A 100 ml Schlenk was charged with 0.2 g (0.4 mmol) of **2** in a mixture of THF (3 ml) and EtOH (15 ml). To this solution was added 0.06 g (0.82 mmol) of solid malanonitrile and four drops of piperidine. An immediate color change from light orange to dark red was observed. The mixture was stirred at r.t. for 1 h, and the solvents were removed in vacuum. The red sticky residue was dissolved in 5 ml of methylene chloride and passed through a silica gel column (25 × 2 cm), and the red band was eluted with 90:10 methylene chloride–hexane mixture. Evaporation of the solvent yielded the red solid of **3** (0.145 g, 0.24 mmol 60% yield). m.p. 170–172 °C. Anal. Calc. for C$_{34}$H$_{30}$FeN$_4$Si$_2$: C, 67.32; H, 4.98; N, 9.24. Found: C, 66.72; H, 5.13; N, 9.21%. ^{1}H-NMR

(CDCl$_3$): 0.51 (s, 6H, SiMe$_2$); 4.06 (t, $J = 1.5$ Hz, 2H, Cp), 4.29 (t, $J = 1.5$ Hz, 2H, Cp); 7.58–7.61 (dd, 2H, Ph), 7.75–7.78 (dd, 2H, Ph), 7.69 (s, 1H, CH=C); ^{13}C-NMR (CDCl$_3$): −1.72 (SiMe$_2$); 69.0 (ipso), 72.4, 73.8 (Cp); 83.2 (CH=C); 113.0, 114.2 (=C(CN)$_2$); 128.9, 131.4, 135.1, 149.7 (Ph), 160.4 (CH=C); ^{29}Si-NMR (CDCl$_3$): −6.0; UV–vis (CH$_2$Cl$_2$): λ_{max} 436 nm.

3.4. Electrochemistry

Electrochemical studies were performed with a 263A Princeton Applied Research potentiostat in 10^{-3} M CH$_2$Cl$_2$ solution with tetrabutylammonium tetrafluoroborate (0.1 M) as supporting electrolyte in a cell equipped with platinum working electrode, and an Ag | AgCl (saturated NaCl) reference electrode and counter electrode.

3.5. NLO measurements

The quadratic hyperpolarizability (β) of **3** was measured in solution by the electric field induced second-harmonic generation (EFISH) technique as described previously [4].

3.6. Mössbauer spectra

The Mössbauer spectra were obtained at 78 and 295 K on a constant-acceleration spectrometer which used a r.t. rhodium matrix cobalt-57 source and was calibrated at r.t. with alpha-iron foil. The spectra have been fit with one or two quadrupole doublets and the resulting isomer shifts and quadrupole splittings are accurate to ± 0.005 and ± 0.01 mm s^{-1}, respectively.

3.7. EPR measurements

Solution and frozen glass EPR spectra were measured at X-band (~ 9.3 GHz) using a Bruker EMX spectrometer. The r.t. (300 K) solution spectra were measured in CH$_2$Cl$_2$. For the low temperature measurements, a 1:1 toluene–CH$_2$Cl$_2$ mixture was used as a glassing solvent, and the temperature was held at 77 K in a nitrogen Dewar.

3.8. X-ray crystal structures for 1 and 3

Two orange crystals of approximate dimensions $0.80 \times 0.48 \times 0.28$ mm (**1**), $0.60 \times 0.32 \times 0.28$ mm (**3**) were mounted on glass fibers in a random orientation. Intensity data were collected at r.t. using a Siemens/Bruker four circle diffractometer with graphite-monochromated Mo–K$_\alpha$ radiation; $\lambda = 0.71073$ Å. Unit cell parameters and standard deviations were obtained by least-squares fit of 25 reflections randomly distributed in reciprocal space in the 2θ range of 15–30°. The ω-scan

technique was used for intensity measurements in all cases. A range of 1.2° in ω was used for **1** and **3**. A variable speed of 4.00 to 20.00 ° min^{-1} was used for compound **1** whereas for **3** this range was 1.4 due to the higher background present in this case. Background counts were taken with stationary crystal and total background time to scan time ratio of 0.5. Three standard reflections were monitored in all cases every 197 reflections and showed no significant decay. The data were corrected for Lorentz and polarization effects and a semi-empirical absorption correction was also applied to each data set giving a Min./Max. transmission ratio of 0.009/0.027 for 1 and 0.100/0.113 for **3**.

Compound **1** is centrosymmetric, space group No. 14, $P2_1/n$ but compound **3** is non-centric, space group No. 9, Cc, therefore Friedel paired reflections were collected to determine the correct absolute structure of the asymmetric unit. All structures were solved by direct methods and refined using the PC-version of the SHELXTL PLUS crystallographic software by Siemens. Full-matrix least-squares refinement of F^2 against all reflections was carried out with anisotropic thermal parameters for non-hydrogen atoms. Hydrogen atoms were placed at calculated positions (C–H = 0.96 Å; $U_H = 0.08$) during refinements. The weighing scheme has the form $w^{-1} = \sigma^2(F_o^2) + (aP)^2 + bP$, where P is $[2F_c^2 + \text{Max}(F_o^2, 0)]/3$. and the final R factors the form $R_1 = \Sigma|F_o - F_c|/\Sigma F_o$ and $R_{w2} = \{\Sigma[w(F_o^2 - F_c^2)^2/\Sigma[w(F_o^2)^2]\}^{1/2}$, these and some other relevant crystallographic parameters are given in Table 1.

References

[1] (a) N.J. Long, Angew. Chem. Int. Ed. Engl. 34 (1995) 21;
(b) H.S. Nalwa, Appl. Organomet. Chem. 5 (1991) 349;
(c) C.C. Frazier, M.A. Harvey, M.P. Cockerham, H.M. Hand, E.A. Chauchard, C.H. Lee, J. Phys. Chem. 90 (1986) 5703;
(d) L.-T. Cheng, W. Tam, G.R. Meredith, S.R. Marder, Mol. Cryst. Liq. Cryst. 189 (1990) 137;
(e) W. Tam, L.-T. Cheng, J.D. Bierlein, L.K. Cheng, Y. Wang, A.E. Feirling, G.R. Meredith, D.F. Eaton, J.C. Calabrese, J.C. Rikken, ACS Symp. Ser. 455 (1991) 158.

[2] (a) I. Su Lee, S.S. Lee, Y.K. Chung, D. Kim, N.W. Song, Inorg. Chim. Acta 279 (1998) 243;
(b) J.C. Calabrese, L.-T. Cheng, J.C. Green, S.R. Marder, W. Tam, J. Am. Chem. Soc. 113 (1997) 7227;
(c) G. Doisneau, G. Balavoine, T. Fillebeen-Khan, J.-C. Client, J. Delaire, I. Ledoux, R. Loucif, G. Puccetti, J. Organomet. Chem. 421 (1991) 299;
(d) S.R. Marder, J.W. Perry, B.G. Tiemann, W.P. Schaefer, Organometallics 10 (1991) 1896;
(e) J.T. Lin, J.J. Wu, C.-S. Li, Y.S. Wen, K.-J. Lin, Organometallics 15 (1996) 5028;
(f) A. Togni, G. Rihs, Organometallics 12 (1993) 3368;
(g) B.J. Coe, C.J. Jones, J.A. McCleverty, D. Bloor, P.V. Kolinsky, R.J. Jones, Chem. Soc. Chem. Commun. (1989) 1485;
(h) M.E. Wright, E.G. Toplikar, Macromolecules 25 (1992) 6050;
(i) S.K. Hurst, M.G. Humphrey, J.P. Morrall, M.P.C. Cifuentes, M. Samoc, B. Luther-Davis, G.A. Heath, A.C. Willis, J. Organomet. Chem. 670 (2003) 56;
(j) G.G.A. Balavoine, J.-C. Daren, G. Iftime, P.G. Lacroix, E. Manoury, J.A. Delaire, I.M. Fanton, K. Nakatani, S.D. Bella, Organometallics 18 (1999) 21;
(k) K. Roque, F. Barange, G.G.A. Balavoine, J.-C. Daren, P.G. Lacroix, E. Manoury, J. Organomet. Chem. 637–639 (2001) 531;
(l) J. Chiffre, F. Averseng, G.G.A. Balavoine, J.-C. Daren, G. Iftime, P.G. Lacroix, E. Manoury, K. Nakatani, Eur. J. Inorg. Chem. 9 (2001) 2221;
(m) G. Iftime, G.G.A. Balavoine, J.-C. Daren, P.G. Lacroix, E. Manoury, Comtes Rend. Acad. Sci. 3 (2000) 139.

[3] M.L.H. Green, S.R. Marder, M.E. Thompson, J.A. Bandy, D. Bloor, P.V. Kolinsky, R.J. Jones, Nature (London) 330 (1987) 360.

[4] (a) G. Mignani, A. Krämer, G. Puccetti, I. Ledoux, G. Soula, J. Zyss, R. Meyrueix, Organometallics 9 (1990) 2640;
(b) G. Mignani, M. Barzoukas, J. Zyss, G. Soula, F. Balegroune, D. Grandjean, D. Josse, Organometallics 10 (1991) 3660;
(c) G. Mignani, A. Krämer, G. Puccetti, I. Ledoux, J. Zyss, G. Soula, Organometallics 10 (1991) 3656;
(d) G. Mignani, A. Krämer, G. Puccetti, I. Ledoux, G. Soula, J. Zyss, J. Molec. Eng. 1 (1991) 11;
(e) D.S. Chemla, J. Zyss, NLO Properties of Organic Molecules and Crystals, Academic Press, Orlando, FL, 1987;
(f) J. Zyss, in: J.L. Bredas, R.R. Chance (Eds.), Organic Crystals and Quadratic Nonlinear Optics, Kluwer Academic Publishers, Amsterdam, 1990, pp. 545–557.

[5] H.K. Sharma, K.H. Pannell, I. Ledoux, J. Zyss, A. Ceccanti, P. Zanello, Organometallics 19 (2000) 770.

[6] (a) C. Grogger, H. Siegl, H. Rautz, H. Stüger, in: N. Auner, J. Weis (Eds.), Organosilicon Chemistry IV, Verlag Chemie, Weinheim, 2000, p. 384;
(b) C. Grogger, H. Rautz, H. Stüger, Montsch Chem. 132 (2001) 453;
(c) H. Rautz, H. Stüger, G. Kickelbick, C. Pietzsch, J. Organomet. Chem. 627 (2001) 167;
(d) C. Beyer, U. Böhme, C. Pietzsch, G. Roewer, J. Organomet. Chem. 654 (2002) 187;
(e) C. Grogger, H. Fallmann, G. Furpaß, H. Stüger, G. Kickelbick, J. Organomet. Chem. 665 (2003) 186.

[7] I. Haiduc, F.T. Edelmann, Supramolecular Organometallic Chemistry, Wiley VCH, Chichester, 1999.

[8] B.T. Holmes, C.W. Padgett, W.T. Pennington, Acta Crystallogr. Sect. C C58 (2002) o602.

[9] B.T. Holmes, C.W. Padgett, W.T. Pennington, Acta Crystallogr. Sect. C C59 (2003) o114.

[10] S. Boryczka, M.M.A. Schreus, J. Kroon, T.C. Steiner, Acta Crystallogr. Sect. C C56 (2000) 263.

[11] Cambridge Crystallographic Data Base V5.24 Nov 2002. Cambridge Crystallographic Data Center, 12 Union Road, Cambridge CB2 1EZ, UK.

[12] R. Deschenaux, M. Schweissguth, M.T. Vilches, A.M. Levelut, D. Hautot, G.J. Long, D. Luneau, Organometallics 18 (1999) 5553.

[13] M.S. Wrighton, M.C. Palazzotto, A.B. Bocarsly, J.M. Bolts, A.B. Fischer, L. Nadjo, J. Am. Chem. Soc. 100 (1978) 7264.